

EFFECTIVE PLASMA BUFFET AND DRAG CONTROL FOR LAMINAR TRANSONIC AIRFOIL

Pavel A. Polivanov*, Andrey A. Sidorenko*

* Khristianovich Institute of Theoretical and Applied Mechanics SB RAS
630090, Institutskaya, 4/1, Novosibirsk, Russia

Keywords: *flow control, transonic, separation, plasma*

Abstract

The effect of plasma actuators on Shock Wave / Laminar Boundary Layer Interaction (SWBLI) was studied experimentally on transonic laminar airfoil. Two kinds of electrical discharge actuators were used for the flow control. Successful suppression of separated flow and laminar transonic buffet by plasma actuators was demonstrated. An analysis of the effect of power and frequency of the discharge on SWBLI was carried out. High efficiency ratio of the separation control by plasma actuators was achieved in the experiments.

1 Introduction

It is commonly accepted that laminar transonic aerofoil should allow to significantly improve the efficiency of transonic aircraft of the next generation. However the features of flow separation at the shock wave / laminar boundary layer interaction (SWBLI) are significantly different from the turbulent cases and not well studied. For example, in papers [1, 2] the characteristics of a laminar transonic aerofoil were studied and natural laminar-turbulent transition was detected in the separation bubble for wide range of the angle of attack. The turbulization of the boundary layer inhibited the growth of the laminar bubble, which positively affects the aerofoil performance. The mode of transonic buffet for a laminar regime is featured by smaller amplitude and a significantly higher frequency of the shock wave oscillations in comparison with the turbulent case. In more detail, the physics of the phenomenon was studied for the test case of flat plate with

incident oblique shock wave at small supersonic Mach numbers with in [3, 4, 5]. Despite the small differences in these experimental studies, the main results are similar: the turbulent boundary layer does not reduce the drag in the interaction zone; in the laminar bubble pulsations rapidly increase leading to turbulence of the flow; in the laminar bubble complex nonstationary phenomena occur, most probably as a result of the growth of the disturbances due to the intrinsic instability of the separation bubble and shear layer. These conclusions are confirmed by the results of numerical simulation [6, 7].

The analysis reveals that the unsteady phenomena for the laminar case develop differently than for the turbulent one. Therefore, not all methods of the separated flow control developed for transonic turbulent aerofoils [8] can be suitable for laminar aerofoils. In [9] it was proposed to use a turbulator of special type to improve the resistance of the aerofoil to laminar transonic buffet. The numerical simulations confirm the possibility of suppressing the buffet, but at the same time the lifting performance of the aerofoil decreases. To maintain the advantages of a laminar aerofoil it is proposed to make a retractable turbulator but this will greatly complicate the design.

In paper [5] it was found that the minimum size of the zone of SWBLI and low level of pulsations may be achieved if the state of inflow boundary layer corresponds to the beginning of the laminar-turbulent transition (low level of intermittency). Since the electrical discharge may introduce disturbances in the laminar boundary layer with predetermined intermittency, it was decided apply this control

technique and to study the effect of plasma actuators on separated flows on laminar transonic airfoil.

2 Experimental setup

The experiments were performed in wind tunnel T-325 (ITAM SB RAS) for Mach number $M_\infty = 0.68-0.72$, $T_0 = 290$ K and $P_0 = 0.3-0.7 \cdot 10^5$ Pa. Figure 1 shows the model installed in the wind tunnel test section. The model was optimized for conditions of the test section of T-325. The main purpose of optimization was to reduce the influence of the sidewalls and to maximize the model chord to improve the accuracy of quantitative measurements. As the base point of optimization of the model shape we have chosen the transonic NLF airfoil [10]. During the numerical optimization process more than 10 configurations of the experimental models were considered.

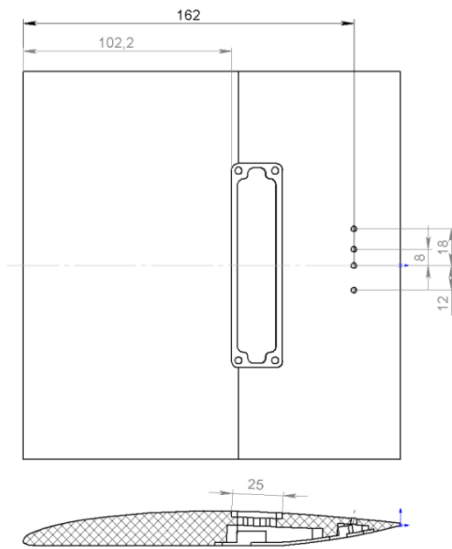


Fig. 1. Photo and draft of the model

The following measuring methods were used: PIV, unsteady pressure sensors, high-

speed Schlieren and IR visualization. Detailed measurements of steady and unsteady characteristics of the separation zone were performed. Two new types of plasma actuators have been developed: MSSD (Multi Sliding Spark Discharge) and CDBD (Contracted Dielectrical Barrier Discharge). Schematically MSSD and CDBD configurations are shown in Figure 2. CDBD is a new plasma actuator specially designed for the introduction of disturbances in the boundary layer. This discharge may be simply integrated into the aircraft structure, operating at moderate voltage and does not require expensive/heavy power supplies.

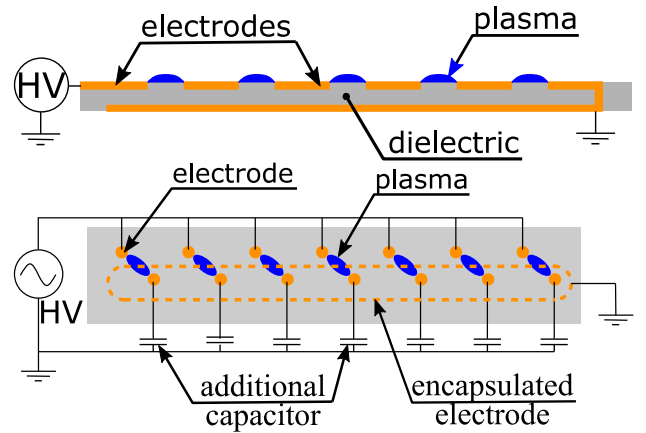


Fig. 2: Schematic of MSSD (top) and CDBD (bottom)

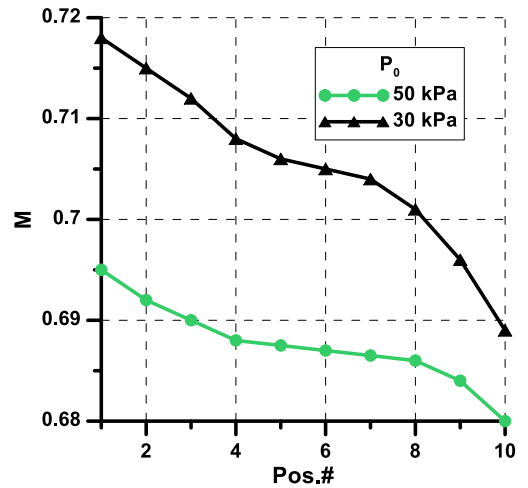


Fig. 3. Free stream Mach number vs. elliptic shaft position

To ensure smooth contours of the model the actuators were milled by CNC from MACOR and the models body was made of PEEK. Sensors Honeywell SCCP15GSMT were used to measure the pressure fluctuations on the

wall. The sensors were placed in-line on the same distance from the leading edge ($x = 162$ mm) to study 3D features of the shock wave oscillations.

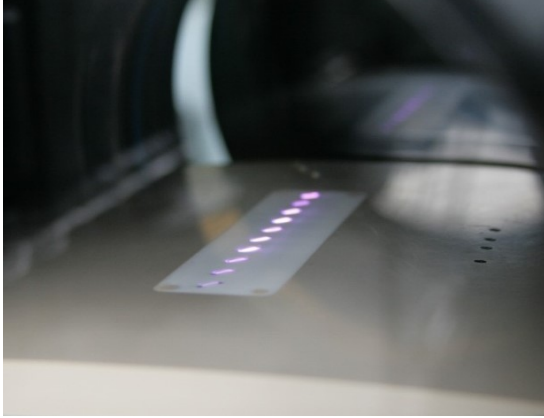
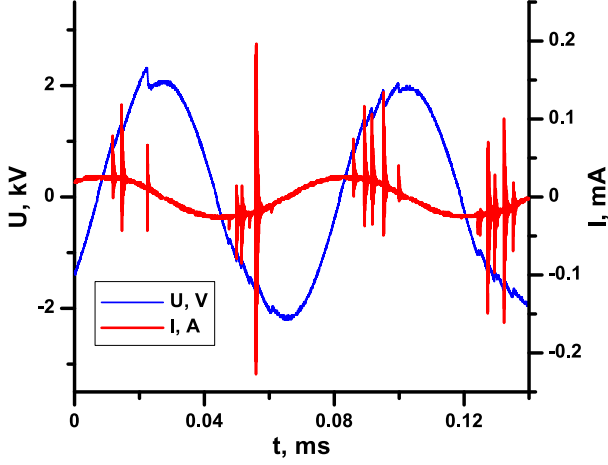


Fig. 4. Waveforms of the voltage and current on CDBD actuator and photo of the actuator

Free stream Mach number was calculated basing on the total pressure P_0 and the static pressure P_{st} measured on the test section wall upstream of the model. These data are presented in Figure 3 for various positions of the elliptic shaft controlling the second throat section of the test chamber. It can be seen that free stream Mach number value was about 0.7 and slightly increased with decreasing of pressure.

Waveforms of current and voltage measured on CDBD actuator are shown in Figure 4. Comparison of these waveforms with the waveforms of classical DBD shows that the breakdown (sharp spikes of the current) occurs much rarely due to fine tuning of the breakdown conditions for each gap by additional capacitor. In fact, the breakdown for each individual electrode pair occurs twice for the period, but due to some differences of discharge gaps

characteristics and local conditions the breakdowns of all the gaps are not simultaneous.

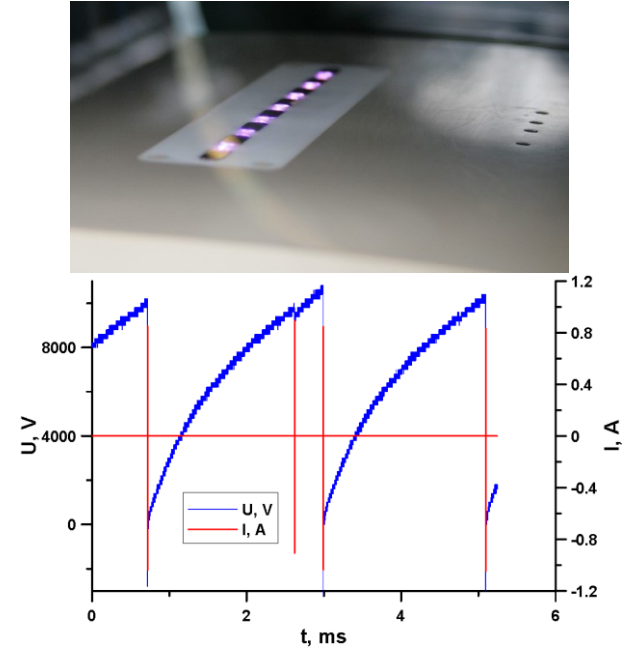


Fig. 5. Waveforms of MSSD voltage and current and photo of the actuator

Example of current and voltage waveforms obtained for MSSD is shown in Figure 5. From the figure one can see the regions of voltage rise corresponding to accumulation of the energy in the capacitor battery and sudden breakdown of the discharge gap. It also can be seen that the charge time is approximately constant. The measured value of time duration of the discharge is $\approx 1-2 \mu s$ that is much lower than any characteristic time of the system. Therefore, it can be assumed that the energy release is instant. The discharge frequency decreases weakly with increasing of the capacity so the average power is increased because of higher pulse energy. The DC HV source allowed to achieve the energy per pulse up to the level typical for CDBD. Therefore, the data for both actuators may be compared.

3 Experimental results

3.1 CDBD actuator

An example of the visualization demonstrating the plasma discharge effect on the flow is

presented in Figure 6 and Figure 7. Activation of CDBD leads to substantial reduction of the separation zone. Analysis of the Schlieren series and the corresponding distributions of Schlieren intensity pulsations did not reveal the formation of turbulent spots by the discharge. This means that CDBD actuator used in the experiment excites perturbations in the boundary layer, insufficient for sudden flow turbulization.

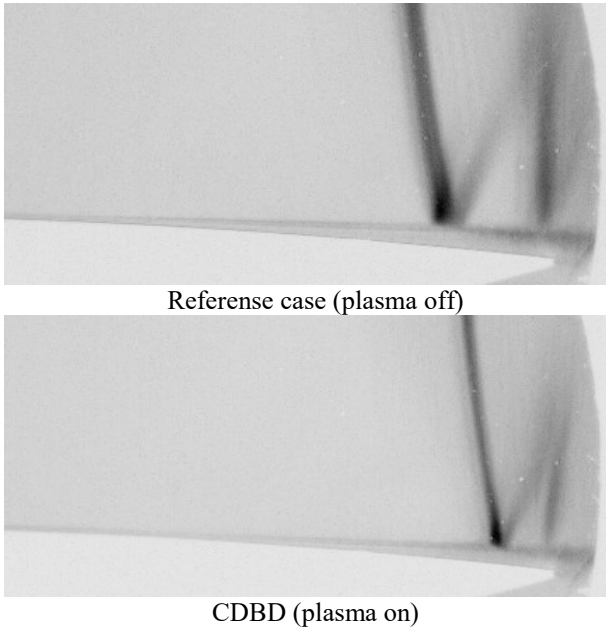


Fig. 6. RMS of the Schlieren image intensity pulsations ($P_0 = 0.3$ bar, shaft position #1)

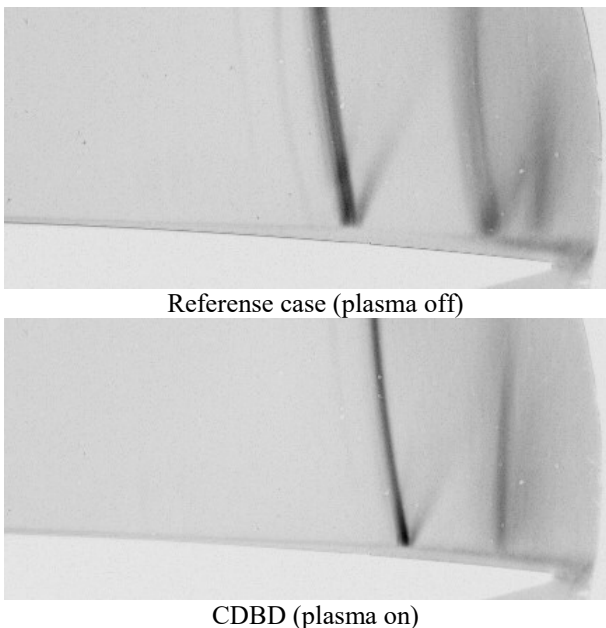


Fig. 7. RMS of the Schlieren image intensity pulsations ($P_0 = 0.3$ bar, shaft position #2)

However, there is rapid growth of these disturbance in the zone of adverse pressure gradient and the shear layer, leading to earlier turbulization of the boundary layer, and consequently to reduction of the separation zone. It is necessary to note that no thermal spots were found in the Schlieren visualization. It means that the negative impact of such direct heat deposition in the flow is minimal. A significant reduction in the separation zone by activation of CDBD was allowed to suppress the laminar transonic buffet.

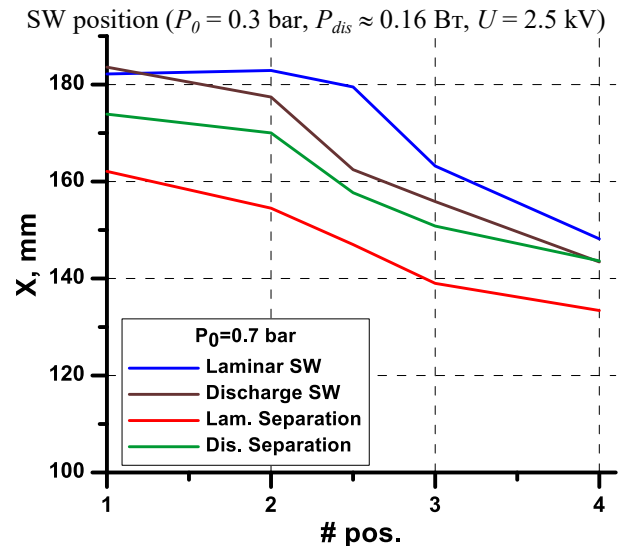
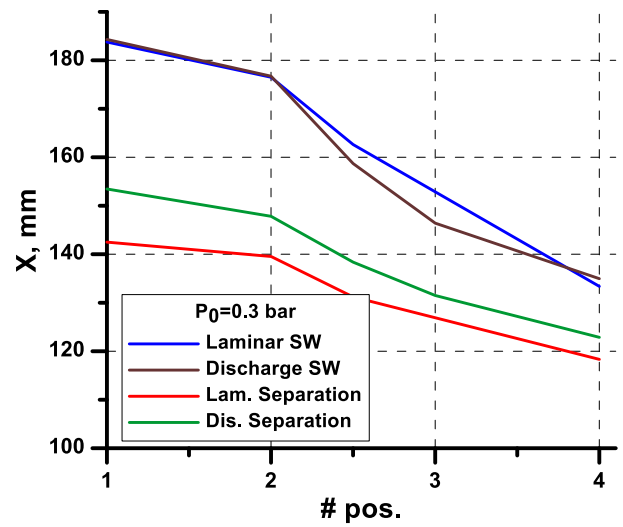


Fig. 8. Effect of upstream Mach number on SW position (CDBD, $f = 13.4$ kHz)

Effect of CDBD on the separated flow for different upstream Mach numbers is shown in Figure 8. The position of the shock wave (SW) and the point of the flow separation was found

from the Schlieren visualization. Since for the laminar case the wave structure consists of several shock waves, only the position of the final shock wave was taken into account in the processing. Activation of CDBD leads to a weak shift of the final shock wave upstream. Experiments with MSSD have been carried out in a wider range of pulse energy. The use of a powerful discharge allowed to rapidly turbulize the flow. As a result, the separated flow was completely suppressed, but the final shock wave shifted significantly upstream. This means that low-power CDBD should lead to more favorable distribution of pressure on the wing surface.

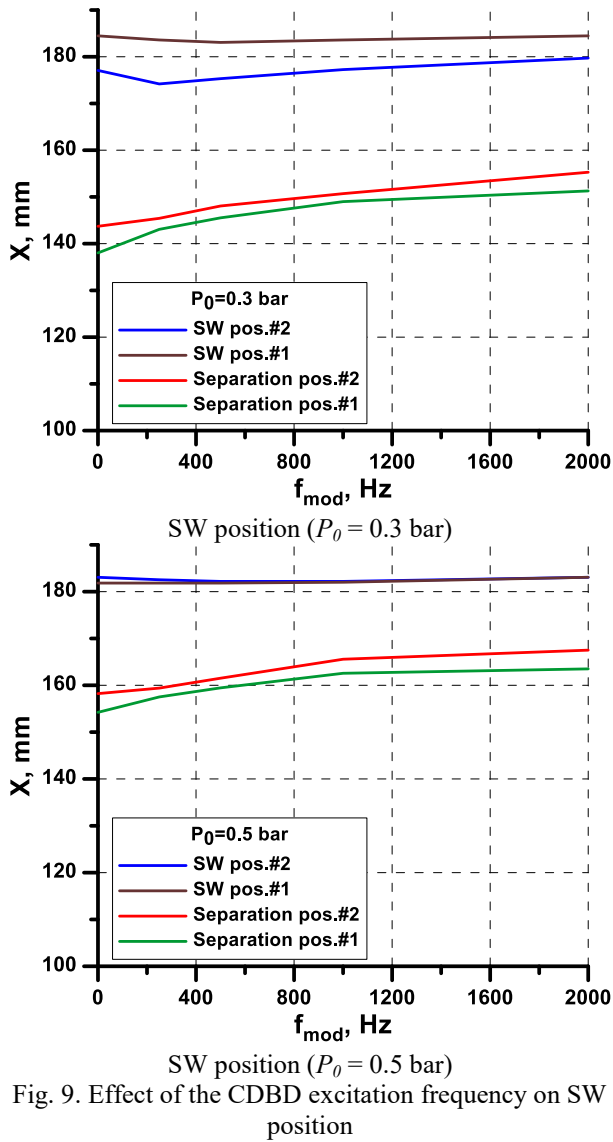


Fig. 9. Effect of the CDBD excitation frequency on SW position

Increasing the pressure from $P_0 = 0.3$ bar to 0.7 bar leads to substantial decrease of the

separation zone with significant corresponding upstream shift of the final shock wave. This is a result of higher discharge power due to increased breakdown voltage with pressure rise and correspondingly more powerful excited disturbances. Most likely, this leads to more rapid origination of turbulence in the zone of adverse pressure gradient. Significant reduction of separation leads to the disappearance of weak compression waves that might reduce the intensity of the final shock wave. Therefore, complete disappearance of the laminar flow separation is not optimal. Rather, there is an optimum of the discharge energy for each test case but the data do not allow to define it.

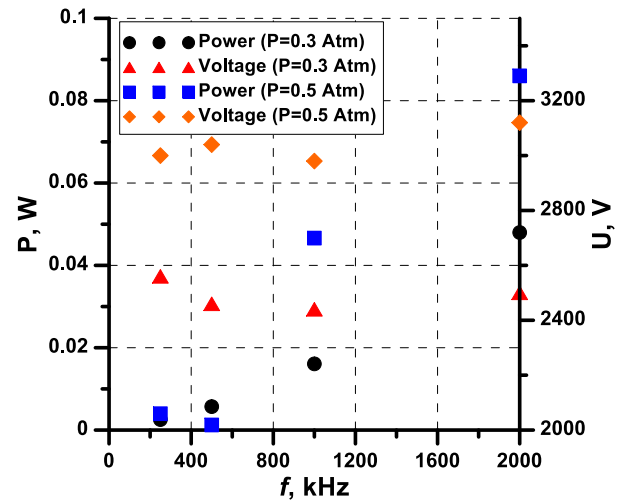


Fig. 10. Discharge parameters at study the effect of the CDBD excitation frequency on SW position

Effect of the excitation frequency (in the range of characteristic interaction frequency) for two P_0 and two shaft positions is shown in Figure 9. An increase of the control efficiency with the frequency rise can be seen in the figure. Beyond the frequency $f_{mod} = 2$ kHz there is not any improvement the flow. Thus, it can be concluded that generation of the perturbations at a frequency of 3-4 times greater than the characteristic frequency of the interaction is sufficient for the control with minimum energy consumption. For example, for the test case of $P_0 = 0.3$ bar it is sufficient to use an average discharge power of 0.5 W/m.

The results presented in Figure 10 for low frequencies of 250 Hz and 500 Hz reveals the false trends, namely the constant power for continuously decreasing frequency, etc. The

reason for this effect is bad statistics of the data acquisition.

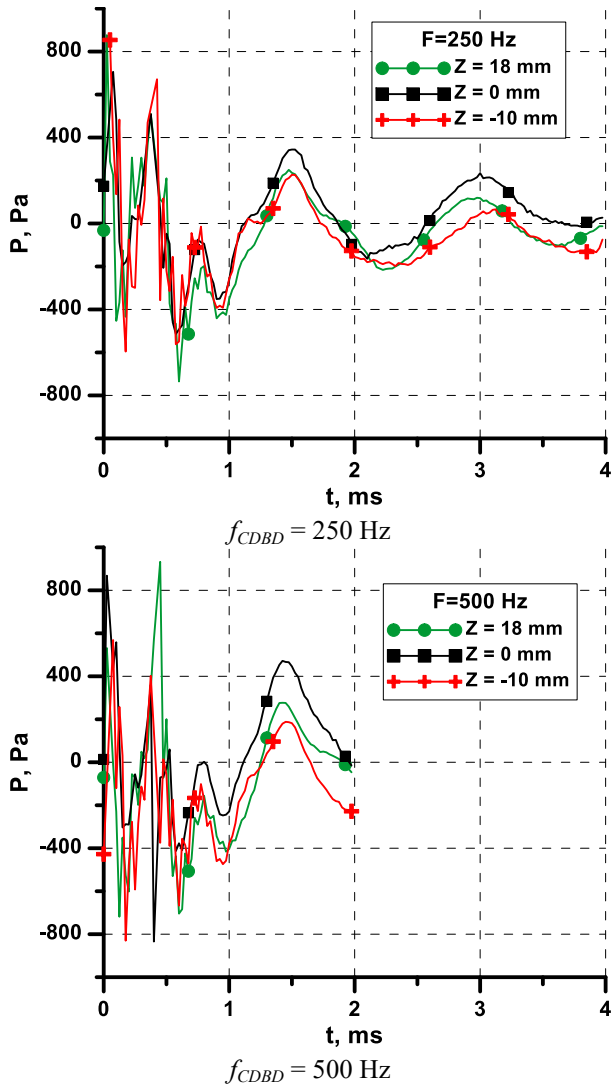


Fig. 11. Waveform of the wall pressure (synchronized, averaged, $P_0 = 0.3$ bar, Shaft position #2)

Evolution of the separated flow after passing of a disturbance may be studied using the information obtained for the cases of low frequency excitations. The pressure waveforms averaged through 500 cycles are presented in Figure 11. The presence of apparent periodicity additionally proves good repeatability of unsteady processes after passing of the disturbance.

During the discharge breakdown the noise does not allow to determine the pressure at the wall for 0.5 ms. Right after this there is a period of negative pressure level indicating absence of the flow separation. After $\Delta t \approx 1$ ms (typical time of the separation recovery) the pressure starts to

increase caused by extending of the separation upstream. As the separation reaches its undisturbed state there is short period of transient regime followed by long period of harmonic oscillations of pressure with constant frequency.

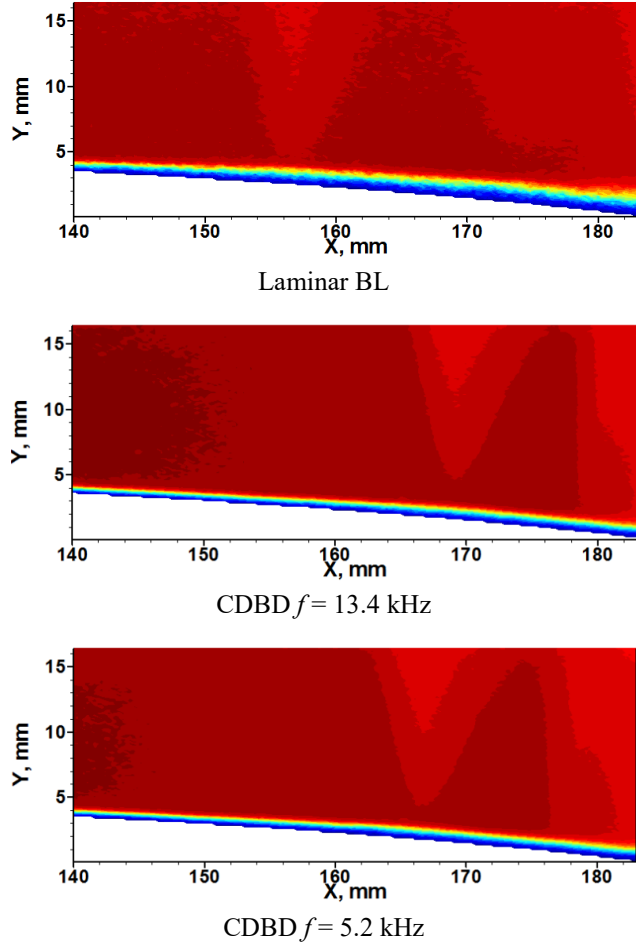


Fig. 12. Time averaged streamwise velocity distributions (shaft position #2, $P_0 = 0.3$ bar)

Increase of the discharge frequency reduces the time window available for the study of unsteadiness but harmonic nature of the oscillations is still evident. These studies were carried out only for the buffet modes (shaft positions #1 and #2). Similar experiments for the modes without harmonic oscillations would clarify the feedback influence on the development of oscillations in the zone of the shock wave / boundary layer interaction.

Figure 12 show the mean velocity distributions obtained for various frequencies (shaft position #2). Similar to the results of Schlieren visualization there were no difference

observed between the cases of $f_{CDBD} = 13.4\text{kHz}$ and 5.2 kHz . Average power of CDBD during PIV measurements for the case of $P_0 = 0.3\text{ bar}$ was 0.25W and 0.5W for the frequencies of 5.2 kHz and 13.4 kHz respectively.

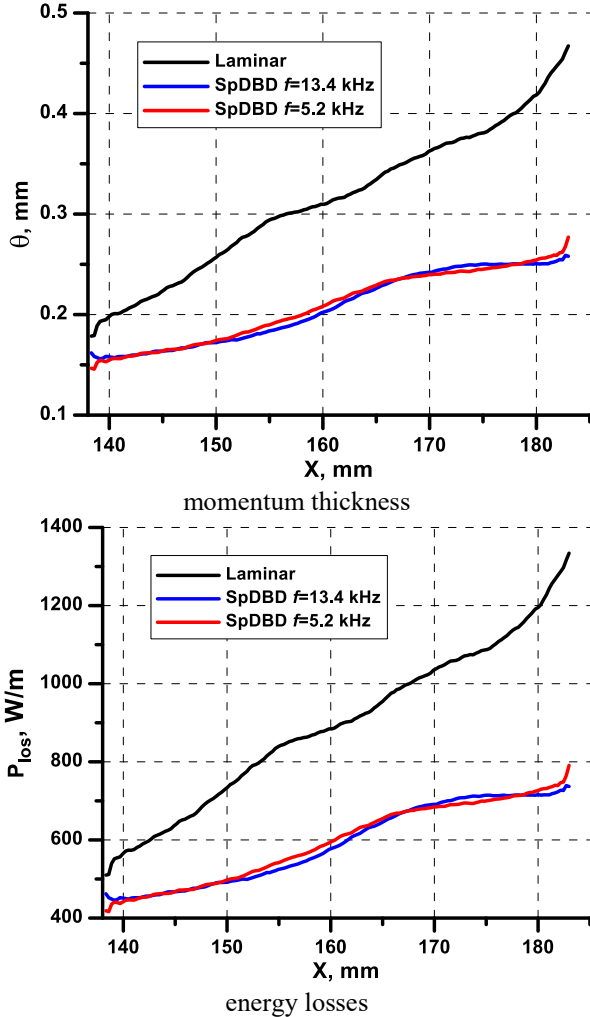


Fig. 13. Streamwise distribution of BL parameters and energy losses (shaft position #2, $P_0=0.3\text{ bar}$)

It can be seen that activation of CDBD reduces the interaction zone, but maintains the flow structure the same. There is the flow acceleration beyond the first shock wave, followed by deceleration to subsonic speed at the final shock wave. These data give evidence that the total boundary layer turbulization does not occur until the end of the model. In the opposite case, the turbulization should significantly increase the boundary layer displacement thickness. This conclusion was confirmed by analysis of the boundary layer velocity profiles. The question about the

mechanism of the interaction control by weak disturbances remains open.

Estimation of the control efficiency in terms of the average flow parameters improvement was done as described below. An estimation of the energy losses (Figure 13) in the interaction may be done basing on changes of the momentum thickness as:

$$P_{los}=0.5\rho\cdot U^3(\theta_{lam}-\theta_{dis}) \quad (1).$$

The curves corresponding to different frequencies of discharge completely coincide.

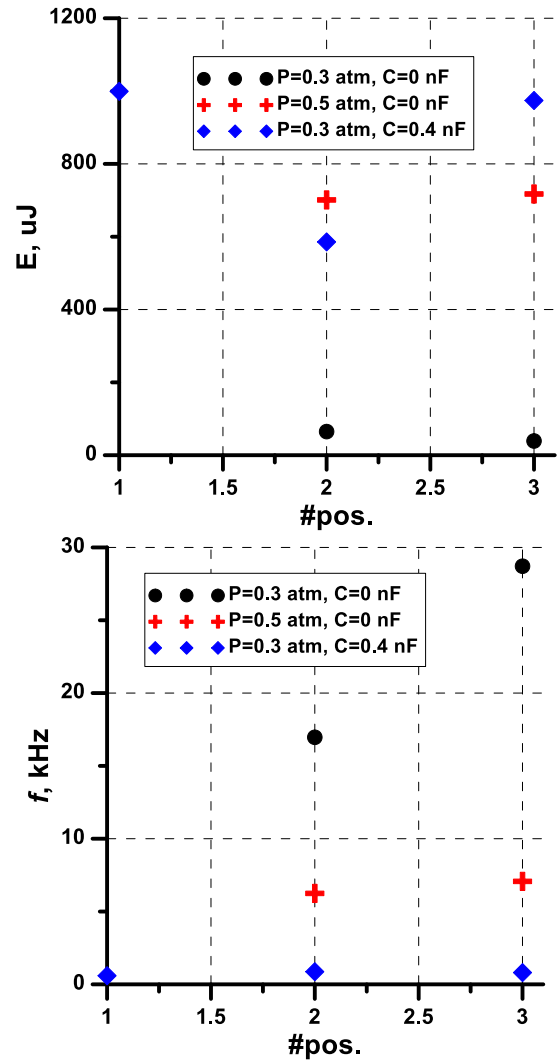


Fig. 14 SSD parameters in the wind tunnel tests (a – Mean energy per pulse, b – Discharge frequency)

Figure 13 show that there is decrease of losses for the cases of plasma control in comparison to laminar reference case along the whole model. PIV data were obtained only for one Mach number (shaft position #2). Therefore, we cannot assert that the same effect would be obtained for lower Mach numbers

where there is some degree of the flow turbulization due to movement of the shock wave upstream.

roughness, vanes and so on) is diminished. Advantages of the turbulence control by plasma turbulators are connected with on-demand using

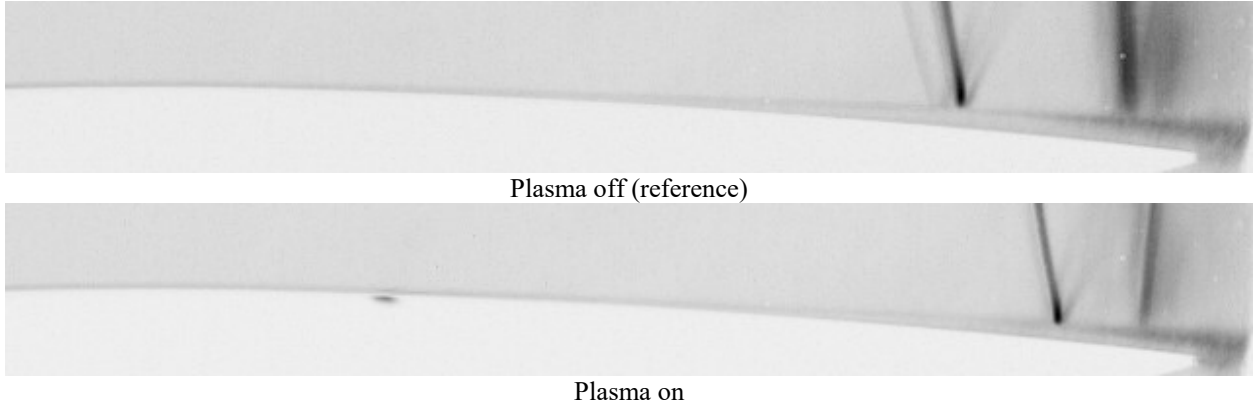


Figure 15 RMS of Schlieren image intensity pulsations (MSSD, $P_0=0.3$ bar)

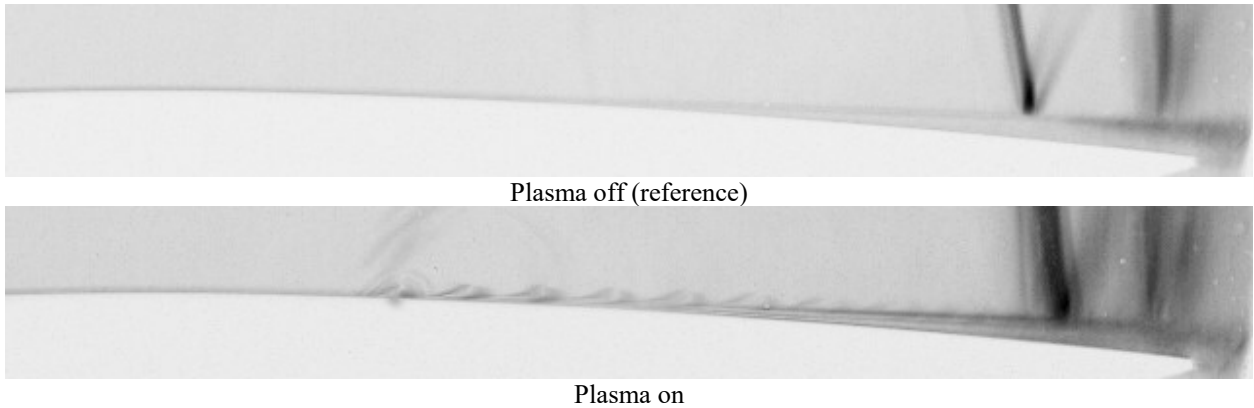


Figure 16 RMS of Schlieren image intensity pulsations (MSSD + capacitor, $P_0=0.3$ bar)

For the case studied, the maximum decrease of P_{los} was achieved near the trailing edge. For the total pressure $P_0 = 0.3$ bar this value is ≈ 550 W/m. Estimation of the control efficiency for the frequency 5.2 kHz gives a result $\eta_{dis} = P_{los}/P_{dis} = 550[\text{W/m}]/(0.25[\text{W}]/0.1[\text{m}]) = 220$ (or 22000%). At the same time, we know from the Schlieren data that the flow pattern remains the same up to discharge frequency of 2 kHz. As a result for the lower frequency the efficiency is even higher $\eta_{dis} = P_{los}/P_{dis} = 550[\text{W/m}]/(0.05[\text{W}]/0.1[\text{m}]) = 1100$ (or 110000 %). Taking into account the output-input ratio of the high voltage generator (about 35%) these values are 77 and 385 for the frequencies 5.2 and 2 kHz correspondingly.

In fact, for so low energy of the discharge its power consumption is negligible. Therefore the main disadvantage of plasma turbulators in front of the classical passive turbulators (such as

and flexible control of the flow by variation of the discharge parameters.

3.2 MSSD actuator

The discharge parameters for the wind tunnel experiments are shown in Figure 14. For the case of $P_0 = 0.3$ bar the value of the average power is comparable to the typical one in CDBD experiments. Since the frequency (20–30 kHz) and the number of discharges are approximately the same, it can be assumed that the energy per pulse is of the same magnitude. This means that the effect of MSSD should be similar to the effect of CDBD. Figure 15 shows distributions of RMS of the Schlieren image intensity pulsations for the cases of active MSSD and without discharge. This figure shows the lack of disturbances in the wake of the discharge, there is only a slight increase in the level of fluctuations near the actuator. This means that, similar to CDBD case, the heat

deposition from this discharge is minimal. The separation behavior is also similar to CDBD in regime of the turbulent spot generation. It only reduces in size but does not completely disappear.

Additional capacitor ($C = 0.4 \text{ nF}$) connected in parallel to the actuator is able to increase the pulse energy by an order but the frequency is reduced up to 500 Hz. For the case of increased energy, Figure 16 shows higher level of the pulsations of the wake behind the actuator as a result of hot and turbulent spots. The average flow pattern is just slightly changed due to low frequency of the discharge activation. However, the analysis of the frame series reveals the flow behavior similar to the case of sliding spark discharge on the Model #2.

The data obtained show that in terms of the effect on the flow the discharge type is not so important. The main question is tuning of discharge parameters and the high voltage source for particular flow conditions. However, in terms of practical implementation CDBD is much preferable as it demands lower voltage and is easier in use especially if implemented on large surfaces. CDBD does not require significant design changes with increasing the discharge gaps number. Moreover, an MSSD requires a complex system of capacitors or large number of power supplies.

Conclusion

Two kinds of plasma actuators were developed and tested for the flow control by exciting the disturbances of low intensity in the flow, particularly Multi Sliding Spark Discharge and Contracted Dielectric Barrier Discharge. The experimental study of the effect of plasma actuators on the SWBLI on a laminar transonic aerofoil was carried out. Possibility of the separation flow control by these actuators has been demonstrated. The separation diminishing and complete elimination was achieved depending on the discharge power. Due to the disturbances generated by the discharge it is possible to achieve suppression of the buffet and to decrease the viscous losses in the zone of SWBLI. High efficiency of the separation

control by plasma actuators was achieved in the experiments. The reasons of this are:

1) Low frequency and low duty cycle of the discharge (short pulse). This is a result the relatively long recovery time of the separation zone.

2) The energy in the pulse was close to the optimum, which is sufficient to generate perturbations at laminar boundary layer without creating a powerful thermal spot.

3) The plasma actuator was operated in single streamer discharge mode. This allows to localize the thermal energy in a small volume and intensify the generation of disturbances [11].

The electric discharge in contrast to the other types of turbulators (such as roughness) can make conditions similar to the beginning of a laminar-turbulent transition (low level of intermittence) along most of the wing surface. This makes it possible to form more favorable conditions for reducing the drag [5] in comparison with the classical turbulator.

The work was supported by grant of RSF 18-19-00547.

References

- [1] V. Brion, J. Dandois, S. Deck, L. Jacquin, P. Molton, Fulvio Sartor and D. Sipp. Transonic airfoil buffet: a decade of research at ONERA. *XXIV ICTAM*, 21-26 August 2016, Montreal, Canada.
- [2] L. Jacquin, V. Brion, P. Molton, D. Sipp, J. Dandois, S. Deck, F. Sartor, E. Coustols, D. Caruana. Testing in Aerodynamics Research at ONERA: the example of the Transonic Buffet. *Journal AerospaceLab*, No.12, 2016.
- [3] M. Diop, S. Piponniau and P. Dupont. On the length and time scales of a laminar Shock Wave Boundary Layer Interaction, *AIAA Paper* 2016-0073, 2016.
- [4] R. H. M. Giepmans, F. F. J. Schrijer, B. W. van Oudheusden. High-resolution PIV measurements of a transitional shock wave-boundary layer interaction. *Exp Fluids* 56:113, p. 20, 2015.
- [5] P.A. Polivanov, A.A. Sidorenko, A.A. Maslov. Transition Effect on Shock Wave / Boundary Layer Interaction at $M=1.47$. *AIAA Paper* 2015-1974, 2015.
- [6] J.-Ph. Boin, J.-Ch. Robinet. Three-dimensional unsteady laminar shock-wave / boundary layer interaction. *NATO RTO-MP-AVT-111*, 2004.
- [7] G. Fournier, A. Chpoun and C. Tenaud. Shedding Intermittency in a Shockwave-Laminar Boundary

- Layer Interaction. *XXIV ICTAM*, 21-26 August 2016, Montreal, Canada.
- [8] A. Lepage, J. Dandois, A. Geeraert, P. Molton, F. Ternoy, J.-B. Dor and E. Coustols. Transonic buffet alleviation on 3D wings: wind tunnel tests and closed-loop control investigations. *Advances in Aircraft and Spacecraft Science*, Vol. 4. No. 2. pp. 145-167, 2017.
- [9] W. Stalewski, J. Sznajder. Load control of natural-laminar-flow wing via boundary layer control. 2016. *VII European Congress on Computational Methods in Applied Sciences and Engineering* M. Papadrakakis, V. Papadopoulos, G. Stefanou, V. Plevris (eds.), ECCOMAS Congress, 2016.
- [10] Natural Laminar flow airfoil analysis and trade studies. *Report NASA-CR-159029*, 1979.
- [11] P.A. Polivanov, A.A. Sidorenko, A.A. Maslov. Artificial turbulization of the supersonic boundary layer by dielectric barrier discharge. *29th Congress of the International Council of the Aeronautical Sciences*, 2014.

Contact Author Email Address

Pavel Polivanov: polivanov@itam.nsc.ru

Andrey Sidorenko: sindr@itam.nsc.ru

Copyright Statement

The authors confirm that they, and/or their company or organization, hold copyright on all of the original material included in this paper. The authors also confirm that they have obtained permission, from the copyright holder of any third party material included in this paper, to publish it as part of their paper. The authors confirm that they give permission, or have obtained permission from the copyright holder of this paper, for the publication and distribution of this paper as part of the ICAS proceedings or as individual off-prints from the proceedings.